

Electronic Supplementary Information

**Cyaphide Group Transfer from Covalent Metal Complexes:
Contrasting Pathways to Transmetallation**

Eric S. Yang^a and Jose M. Goicoechea^{*,b}

^a Department of Chemistry, University of Oxford, Chemistry Research Laboratory, 12
Mansfield Rd., Oxford, OX1 3TA, U.K.

^b Department of Chemistry, Indiana University, 800 East Kirkwood Ave., Bloomington,
Indiana, 47405, U.S.A.

E-mail: jgoicoec@iu.edu

Contents

1. Experimental section.....	2
1.1 General experimental methods	2
1.2 Synthesis of reported compounds	3
1.3 Cyclic voltammetry	12
2. Single crystal X-ray diffraction data	15
3. Computational details	16
3.1. General computational methods	16
3.2. Electronic structure calculations	17
3.3. Topological Analysis.....	21
3.4. XYZ coordinates.....	22
4. References.....	24

1. Experimental section

1.1 General experimental methods

Synthetic methods. Unless specified otherwise, reactions and product manipulations were carried out using standard Schlenk-line techniques under an inert atmosphere of argon, or in a dinitrogen filled glovebox (MBraun UNILab glovebox maintained at < 0.1 ppm H₂O and < 0.1 ppm O₂). Au(IDipp)(CP),¹ Ga(DippNacNac),² and Fe(depe)₂(N₂)³ were synthesised according to previously reported synthetic procedures. Me₃SiCl (98%, Sigma Aldrich) was purchased and used as received. [NBu₄][PF₆] (98%, Sigma Aldrich) was purified by two-fold recrystallization from methanol. Ferrocene (98%, Sigma Aldrich) was purified by vacuum sublimation. Toluene (Sigma Aldrich HPLC grade), benzene (Sigma Aldrich HPLC grade), acetonitrile (Sigma Aldrich HPLC grade), and hexane (Sigma Aldrich HPLC grade) were purified using an MBraun SPS-800 solvent system. C₆D₆ (Aldrich, 99.5%) was degassed dried over CaH₂. All dry solvents were stored under argon in gas-tight ampoules over activated 3 Å molecular sieves.

Characterization techniques. NMR spectra were acquired on a Bruker AVIII 400 MHz NMR spectrometer (¹H 400 MHz, ³¹P 162 MHz), Bruker AVIII 500 MHz NMR spectrometer (¹H 500 MHz, ³¹P 202 MHz) or a Bruker Avance NEO 600 MHz NMR spectrometer with a broadband helium cryoprobe (¹³C 151 MHz). ¹H and ¹³C NMR spectra were referenced to the most downfield solvent resonance (¹H NMR C₆D₆: δ = 7.16 ppm, ¹³C NMR C₆D₆: δ = 128.06 ppm). ³¹P NMR spectra were externally referenced to an 85% solution of H₃PO₄ in H₂O. Raman spectra were acquired on a Thermo Fisher Scientific DXR3 SmartRaman spectrometer using a 532 nm laser. Cyclic voltammetry experiments were performed in a MBraun UNILab glovebox with a PalmSens Emstat3+ Blu potentiostat using a glassy carbon working electrode, a Pt wire counter electrode, and an Ag wire pseudo-reference electrode. Elemental analyses were carried out by London Metropolitan University (London, U.K.). Samples (approx. 5 mg) were submitted in flame sealed glass tubes.

1.2 Synthesis of reported compounds

1.2.1 Synthesis of Au(IDipp){Ga(^{Dipp}NacNac)(CP)} (1)

Au(IDipp)(CP) (18 mg, 0.03 mmol) and Ga(^{Dipp}NacNac) (14 mg, 0.03 mmol) were dissolved in toluene (1 mL) and stirred overnight. The reaction mixture was filtered to remove any particulates, then concentrated and stored at -35 °C for 3 days, yielding colourless needles of Au(IDipp){Ga(^{Dipp}NacNac)(CP)}. The supernatant was decanted, and the crystals were then washed with cold hexane (2 × 0.5 mL) and dried under vacuum. Yield: 25 mg, 0.02 mmol, 78%. Anal. Calcd. (%) for C₅₇H₇₇N₄AuGaP: C, 61.35; H, 6.96; N, 5.02. Found: C, 62.09; H, 7.44; N, 4.64.

¹H NMR (600 MHz, C₆D₆): δ(ppm) 7.28 (t, 2H, ³J_{H-H} = 7.7 Hz, IDipp Dipp *para*-CH), 7.21 (dd, 2H, ³J_{H-H} = 7.6 Hz, ⁴J_{H-H} = 1.6 Hz, NacNac Dipp *meta*-CH), 7.18 (t, 2H, ³J_{H-H} = 7.5 Hz, NacNac Dipp *para*-CH), 7.04 (d, 4H, ³J_{H-H} = 7.8 Hz, IDipp Dipp *meta*-CH), 7.00 (dd, 2H, ³J_{H-H} = 7.5 Hz, ⁴J_{H-H} = 1.6 Hz, NacNac Dipp *meta*-CH), 6.13 (s, 2H, IDipp CH), 4.93 (s, 1H, NacNac CH), 4.26 (sept, 2H, ³J_{H-H} = 6.7 Hz, NacNac Dipp CH(CH₃)₂), 3.34 (sept, 2H, ³J_{H-H} = 6.8 Hz, NacNac Dipp CH(CH₃)₂), 2.39 (sept, 4H, ³J_{H-H} = 6.9 Hz, IDipp Dipp CH(CH₃)₂), 1.58 (s, 6H, NacNac CH₃), 1.42 (d, 6H, ³J_{H-H} = 6.7 Hz, NacNac Dipp CH(CH₃)₂), 1.25 (d, 6H, ³J_{H-H} = 6.7 Hz, NacNac Dipp CH(CH₃)₂), 1.15 (d, 6H, ³J_{H-H} = 6.9 Hz, NacNac Dipp CH(CH₃)₂), 1.09 (d, 12H, ³J_{H-H} = 6.9 Hz, IDipp Dipp CH(CH₃)₂), 0.98 (d, 6H, ³J_{H-H} = 6.9 Hz, NacNac Dipp CH(CH₃)₂).

¹³C{¹H} NMR (151 MHz, C₆D₆): δ(ppm) 251.61 (d, ²J_{C-P} = 20.9 Hz, CP), 214.68 (s, IDipp CAu), 166.56 (s, NacNac CNDipp), 145.95 (s, NacNac Dipp *ortho*-C), 145.61 (s, IDipp Dipp *ortho*-C), 144.91 (s, NacNac Dipp *ortho*-C), 142.90 (s, NacNac Dipp *ipso*-C), 134.95 (s, IDipp Dipp *ipso*-C), 130.33 (s, IDipp Dipp *para*-C), 125.56 (s, NacNac Dipp *para*-C), 124.18 (s, NacNac Dipp *meta*-C), 124.09 (s, IDipp Dipp *meta*-C), 123.23 (s, NacNac Dipp *meta*-C), 122.51 (s, IDipp CH), 97.31 (s, NacNac CH), 30.50 (s, IDipp Dipp CH(CH₃)₂), 28.88 (s, IDipp Dipp CH(CH₃)₂), 28.87 (s, NacNac Dipp CH(CH₃)₂), 27.83 (s, NacNac Dipp CH(CH₃)₂), 25.42 (s, NacNac Dipp CH(CH₃)₂), 25.14 (s, IDipp Dipp CH(CH₃)₂), 24.77 (s, IDipp Dipp CH(CH₃)₂), 24.21 (s, IDipp Dipp CH(CH₃)₂), 23.93 (s, NacNac Dipp CH(CH₃)₂), 23.61 (s, NacNac CH₃).

³¹P{¹H} NMR (162 MHz, C₆D₆): δ(ppm) 109.8 (s, CP).

Raman: 1329 cm⁻¹ (s, ν(C≡P)).

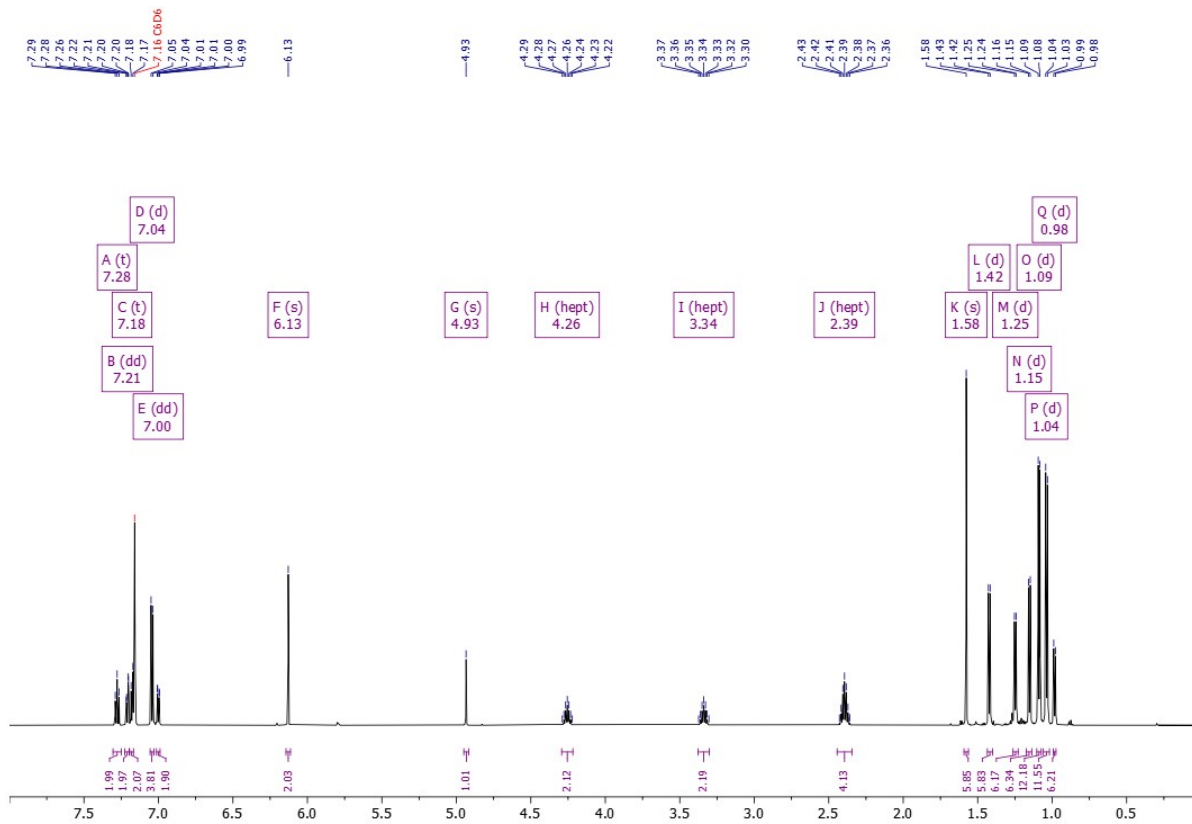


Figure S1. ^1H NMR (600 MHz) spectrum of **1** in C_6D_6 .

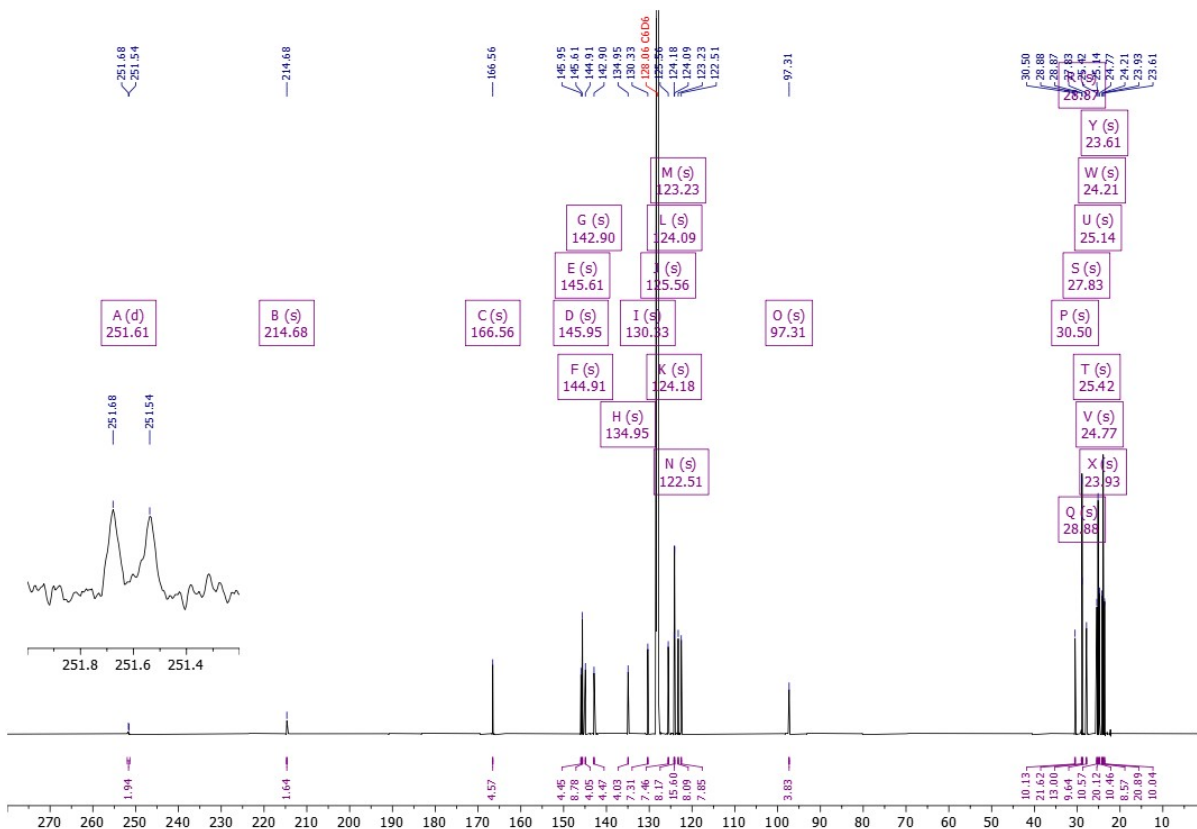


Figure S2. $^{13}\text{C}\{^1\text{H}\}$ NMR (151 MHz) spectrum of **1** in C_6D_6 .

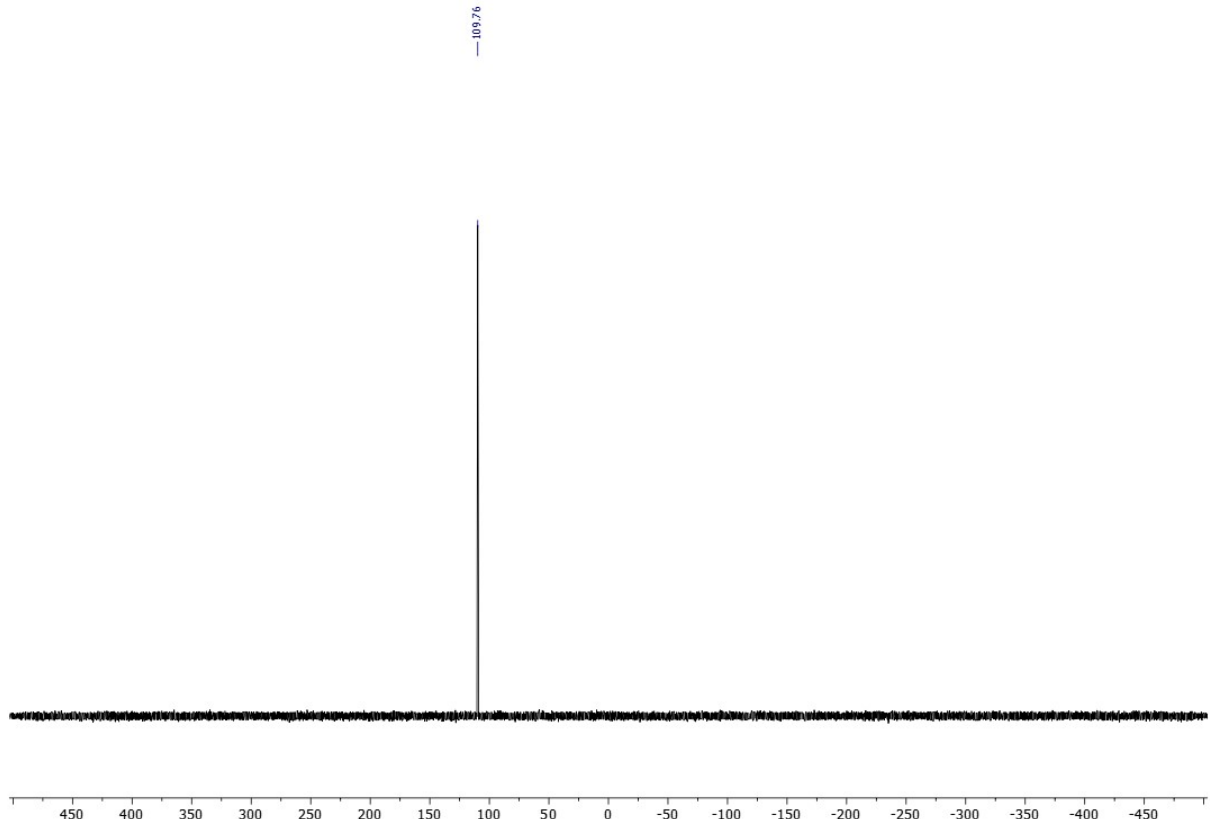


Figure S3. $^{31}\text{P}\{^1\text{H}\}$ NMR (162 MHz) spectrum of **1** in C_6D_6 .

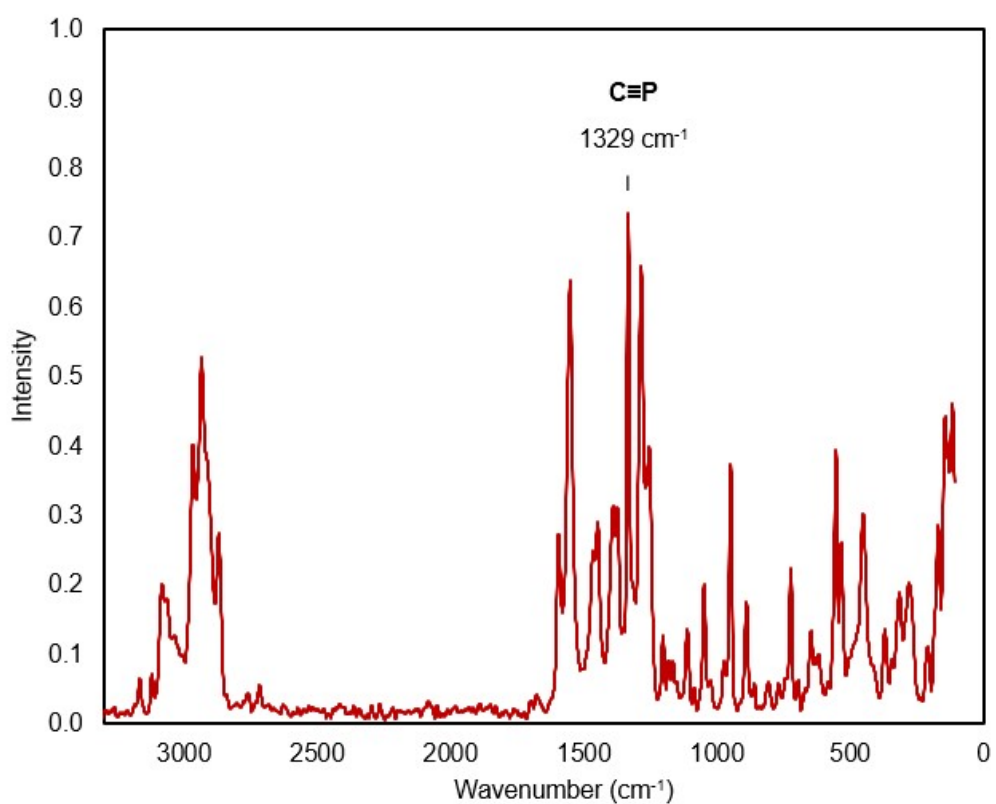


Figure S4. Dispersive Raman spectrum of **1**.

1.2.2 Synthesis of $\{\text{Fe(depe)}_2\}_2(\text{C}_2\text{P}_2\text{Au}_2)$ (2)

$\text{Au}(\text{IDipp})(\text{CP})$ (190 mg, 0.30 mmol) and $\text{Fe}(\text{depe})_2(\text{N}_2)$ (150 mg, 0.30 mmol) were dissolved in benzene (10 mL), then filtered to remove any remaining particulates. The dark orange-red solution was then freeze-pump-thaw degassed, during which vigorous gas evolution is observed on each thaw cycle. The degassed solution was left to stand under a static vacuum for 10 days, during which $\{\text{Fe}(\text{depe})_2\}_2(\text{C}_2\text{P}_2\text{Au}_2)$ crystallizes as red blocks. The supernatant was decanted, then the solvent removed under vacuum. The resulting residue was washed with hexane (2×3 mL), then recrystallized from a toluene/acetonitrile layer to obtain a second crop of product as red needles. The crystalline product was washed with acetonitrile (2×5 mL) then dried under vacuum. Yield: 129 mg, 0.09 mmol, 61%. Anal. Calcd. (%) for $\text{C}_{42}\text{H}_{96}\text{Au}_2\text{Fe}_2\text{P}_{10}\cdot\text{C}_7\text{H}_8$: C, 39.03; H, 6.89; N, 0.00. Found: C, 38.09; H, 6.85; N, 0.00.

$^1\text{H}\{^{31}\text{P}\}$ NMR (500 MHz, C_6D_6): δ (ppm) 3.13–3.00 (m, 2H, PCH_2CH_3), 3.02–2.91 (m, 2H, PCH_2CH_3), 2.88–2.75 (m, 2H, PCH_2CH_3), 2.48–2.37 (m, 2H, PCH_2CH_3), 2.39–2.29 (m, 2H, PCH_2CH_3), 2.30–2.21 (m, 1H, $\text{C}_2\text{H}_4(\text{PEt}_2)_2$), 2.24–2.14 (m, 2H, PCH_2CH_3), 2.05–1.98 (m, 2H, $\text{C}_2\text{H}_4(\text{PEt}_2)_2$), 1.98–1.89 (m, 2H, PCH_2CH_3), 1.87–1.75 (m, 2H, $\text{C}_2\text{H}_4(\text{PEt}_2)_2$), 1.77–1.71 (m, 2H, PCH_2CH_3), 1.72–1.60 (m, 1H, $\text{C}_2\text{H}_4(\text{PEt}_2)_2$), 1.62–1.46 (m, 6H, PCH_2CH_3), 1.46–1.41 (m, 1H, $\text{C}_2\text{H}_4(\text{PEt}_2)_2$), 1.42–1.31 (m, 3H, PCH_2CH_3), 1.29–1.25 (m, 3H, PCH_2CH_3), 1.20–1.12 (m, 1H, $\text{C}_2\text{H}_4(\text{PEt}_2)_2$), 1.11–1.06 (m, 2H, $\text{C}_2\text{H}_4(\text{PEt}_2)_2$), 1.08–0.95 (m, 6H, PCH_2CH_3), 0.88–0.81 (m, 3H, PCH_2CH_3), 0.83–0.73 (m, 3H, PCH_2CH_3),

$^{13}\text{C}\{^1\text{H}\}$ NMR (151 MHz, C_6D_6): δ (ppm) 31.62–30.86 (m, PCH_2CH_3), 30.28–29.63 (m, PCH_2CH_3), 28.92–27.98 (m, PCH_2CH_3), 27.51–26.56 (m, PCH_2CH_3), 25.02–24.16 (m, $\text{C}_2\text{H}_4(\text{PEt}_2)_2$), 23.87–23.48 (m, PCH_2CH_3), 23.43–22.83 (m, $\text{C}_2\text{H}_4(\text{PEt}_2)_2$), 22.23–21.46 (m, PCH_2CH_3), 20.98–19.83 (m, PCH_2CH_3), 15.89–15.21 (m, $\text{C}_2\text{H}_4(\text{PEt}_2)_2$), 15.21–14.53 (m, $\text{C}_2\text{H}_4(\text{PEt}_2)_2$), 11.85–10.98 (m, PCH_2CH_3), 10.31 (s, PCH_2CH_3), 9.99 (s, PCH_2CH_3), 9.72 (s, PCH_2CH_3), 9.57 (s, PCH_2CH_3), 9.10 (s, PCH_2CH_3), 8.94 (s, PCH_2CH_3), 8.68 (s, PCH_2CH_3), 8.58 (s, PCH_2CH_3).

$^{31}\text{P}\{^1\text{H}\}$ NMR (202 MHz, C_6D_6): δ (ppm) 149.3–148.2 (m, CP), 73.1–71.0 (m, $\text{C}_2\text{H}_4(\text{PEt}_2)_2$), 71.0–70.0 (m, $\text{C}_2\text{H}_4(\text{PEt}_2)_2$), 67.3–65.9 (m, $\text{C}_2\text{H}_4(\text{PEt}_2)_2$).

Raman: 1047 cm^{-1} (m, $\nu(\text{C}\equiv\text{P})$), 117 cm^{-1} (m, $\nu(\text{Au}-\text{Au})$).

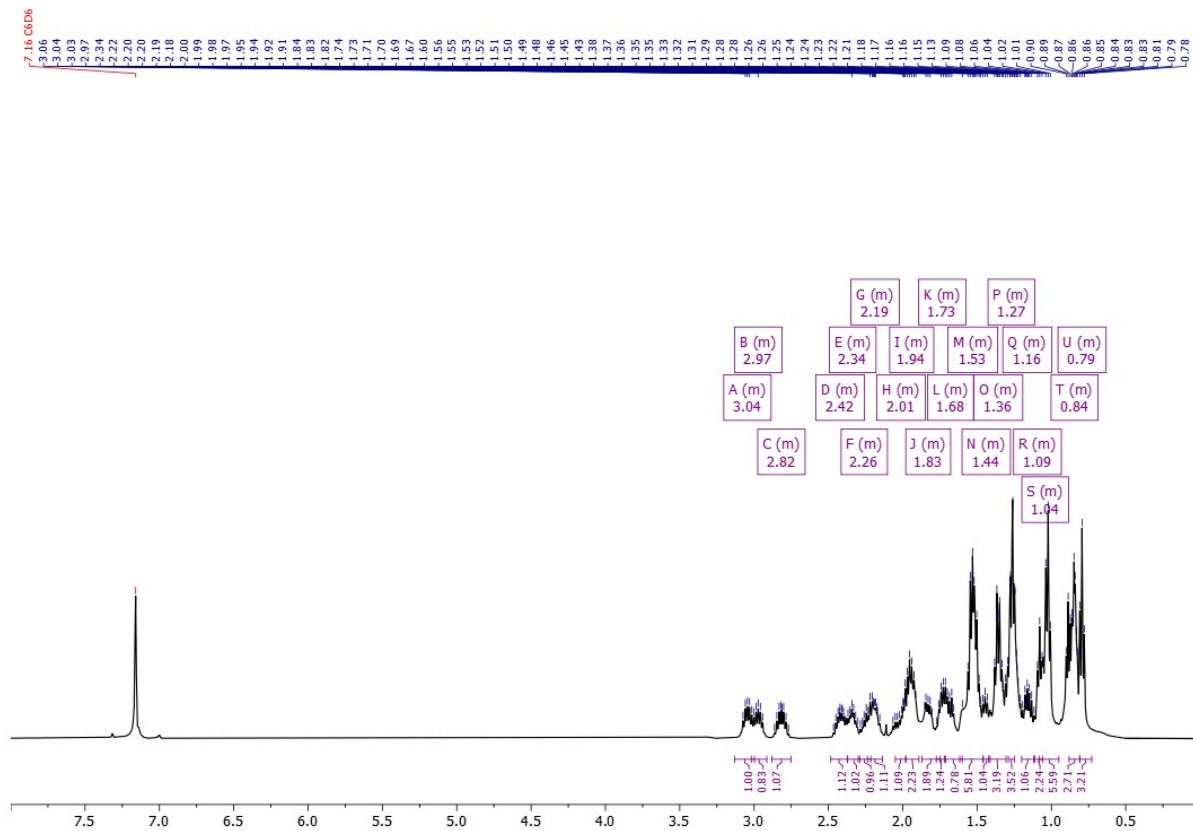


Figure S5. $^1\text{H}\{^{31}\text{P}\}$ NMR (500 MHz) spectrum of **2** in C_6D_6 .

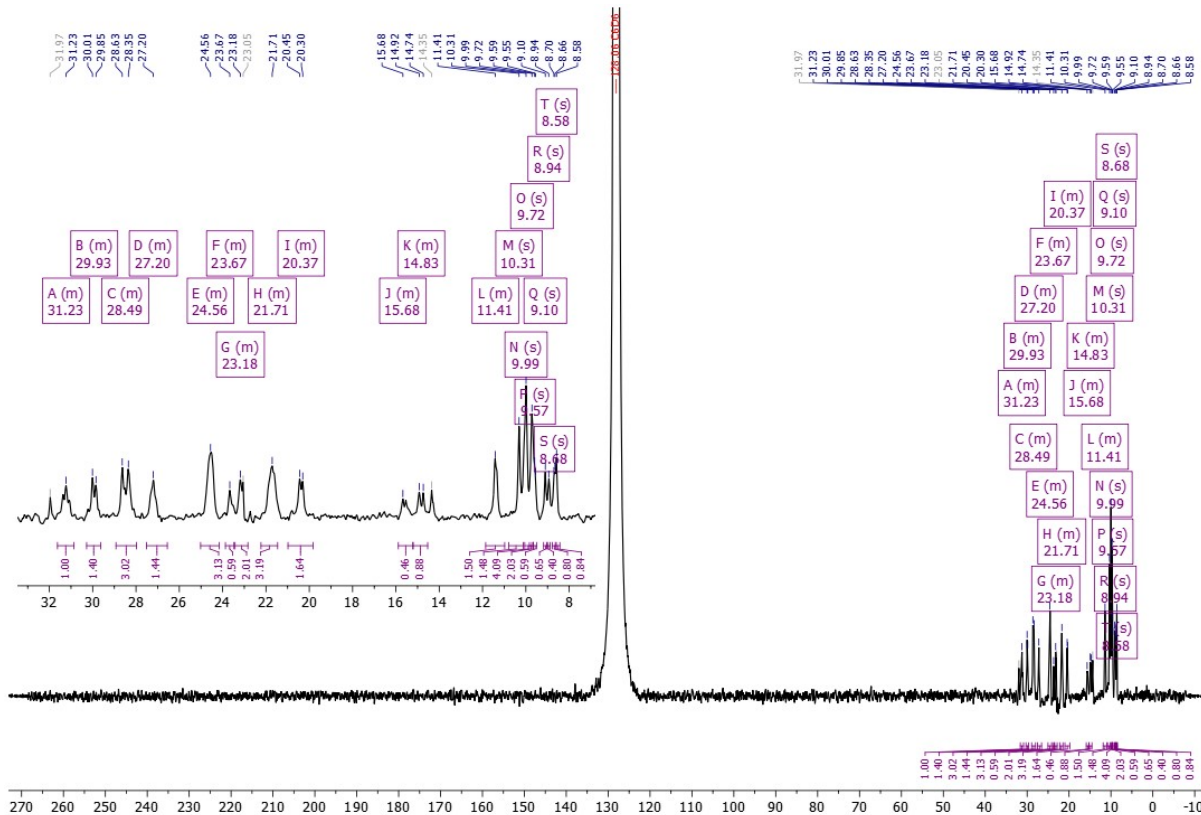


Figure S6. $^{13}\text{C}\{^1\text{H}\}$ NMR (151 MHz) spectrum of **2** in C_6D_6 .

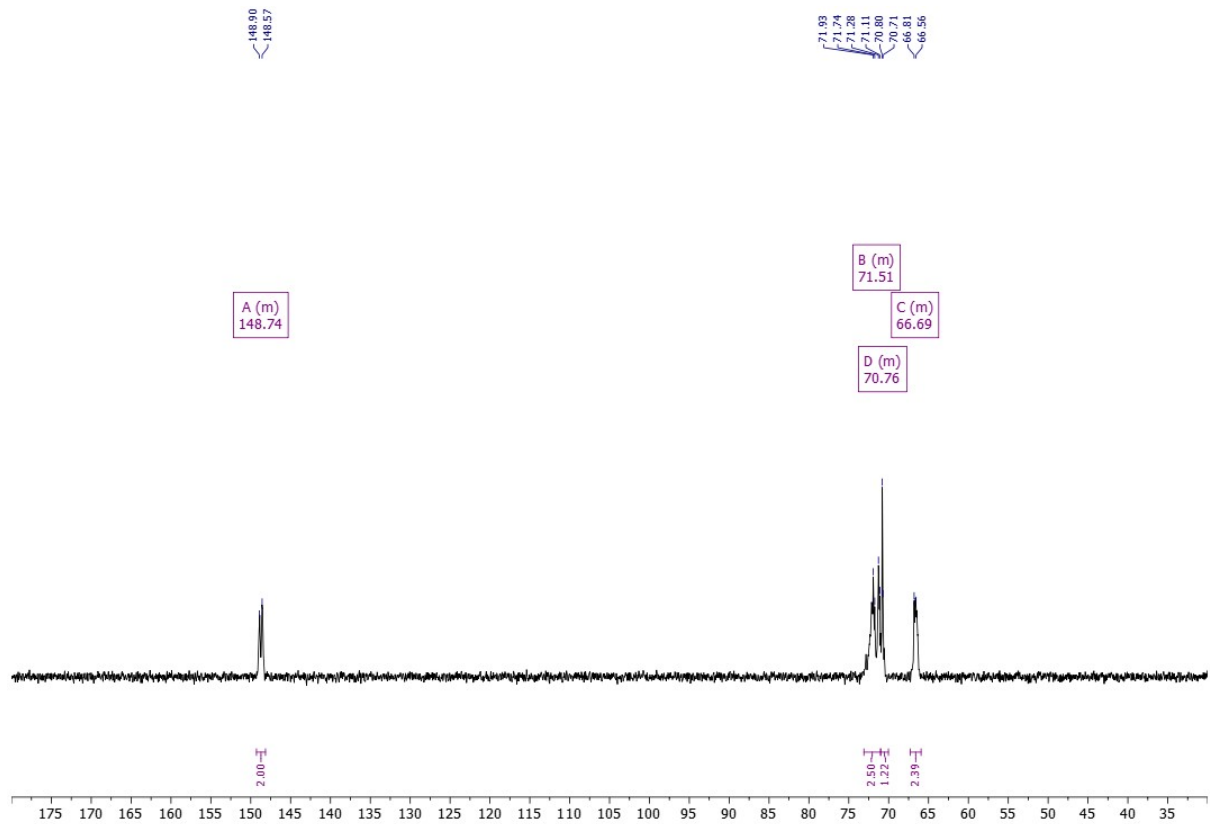


Figure S7. $^{31}\text{P}\{\text{H}\}$ NMR (162 MHz) spectrum of **2** in C_6D_6 .

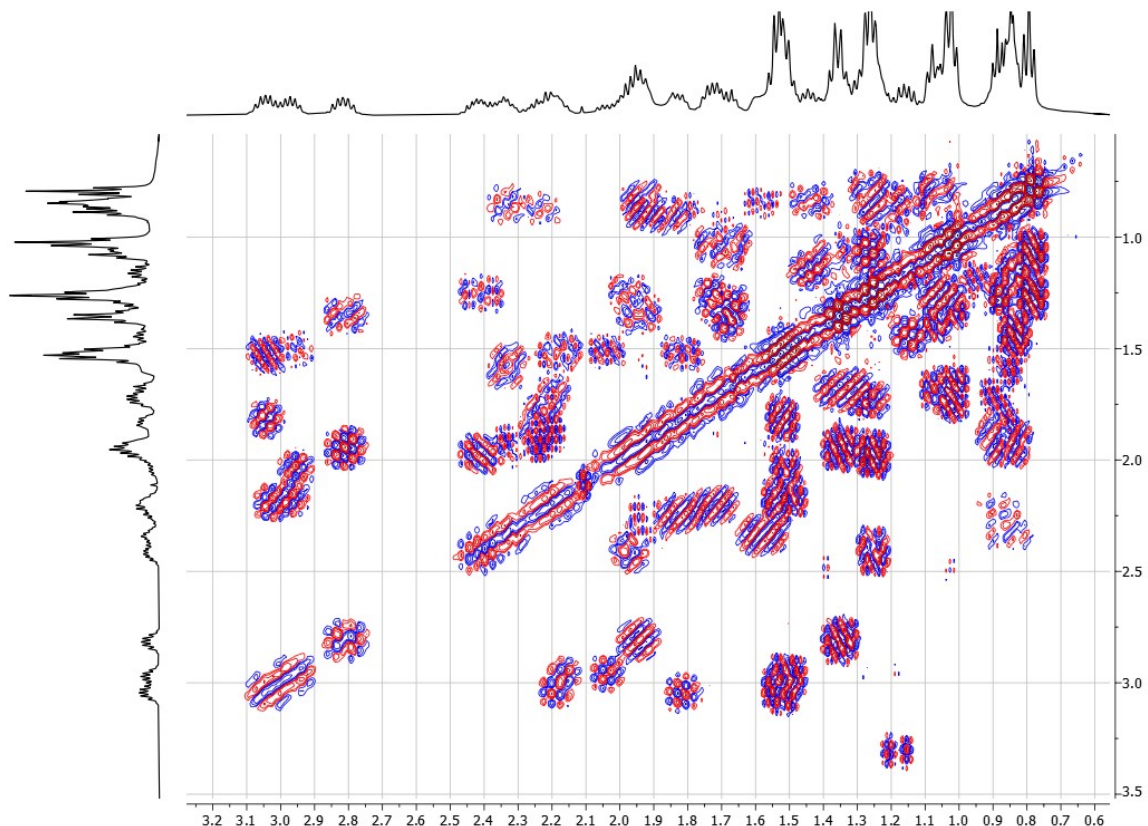


Figure S8. ^1H COSY spectrum of **2** in C_6D_6 .

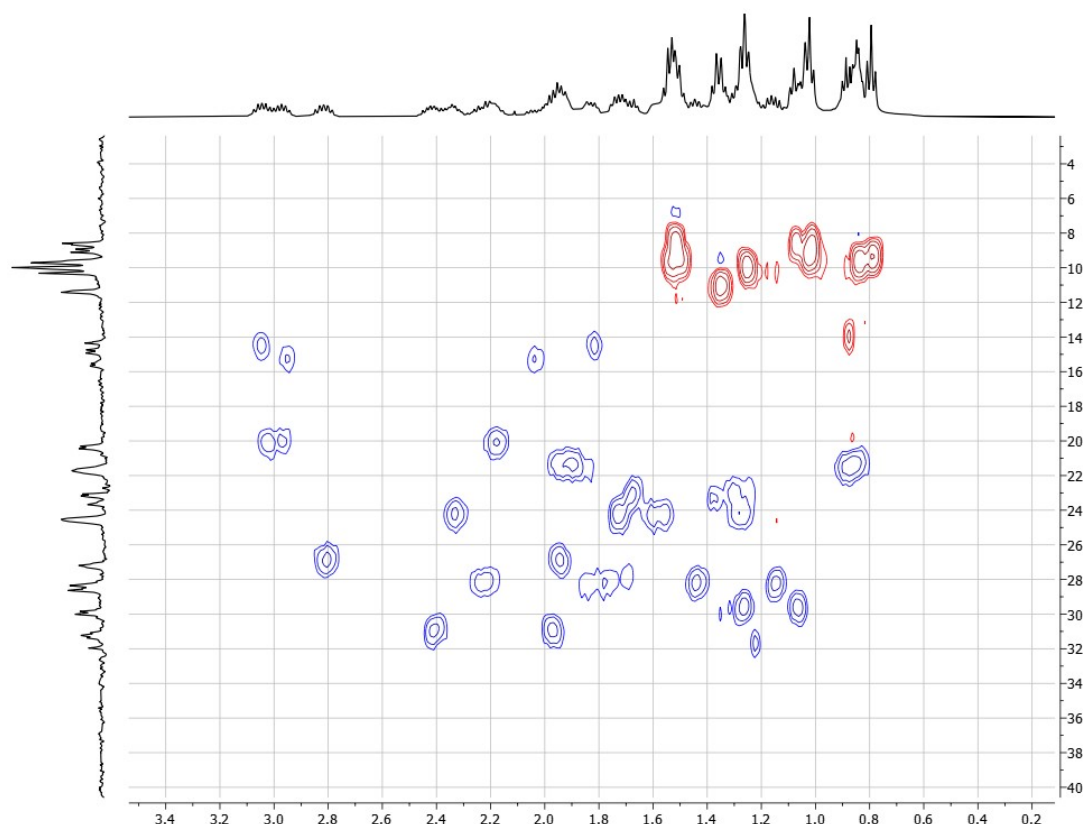


Figure S9. Edited HSQC spectrum of **2** in C_6D_6 .

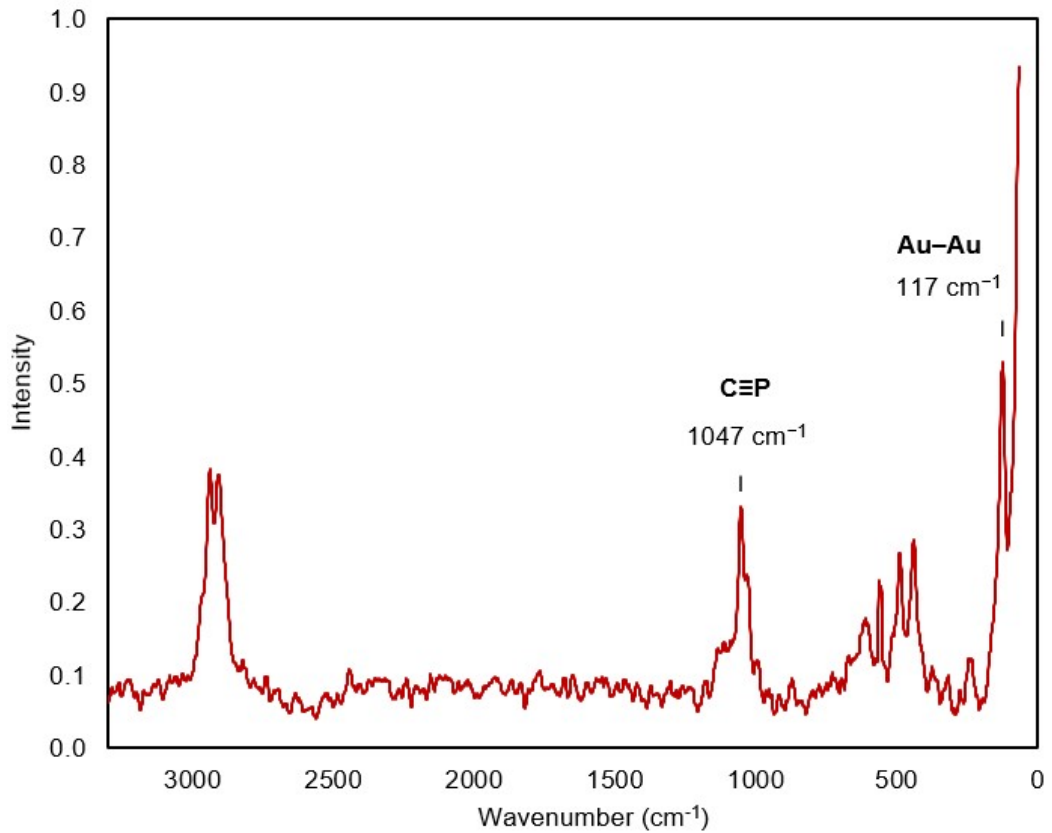


Figure S10. Dispersive Raman spectrum of **2**.

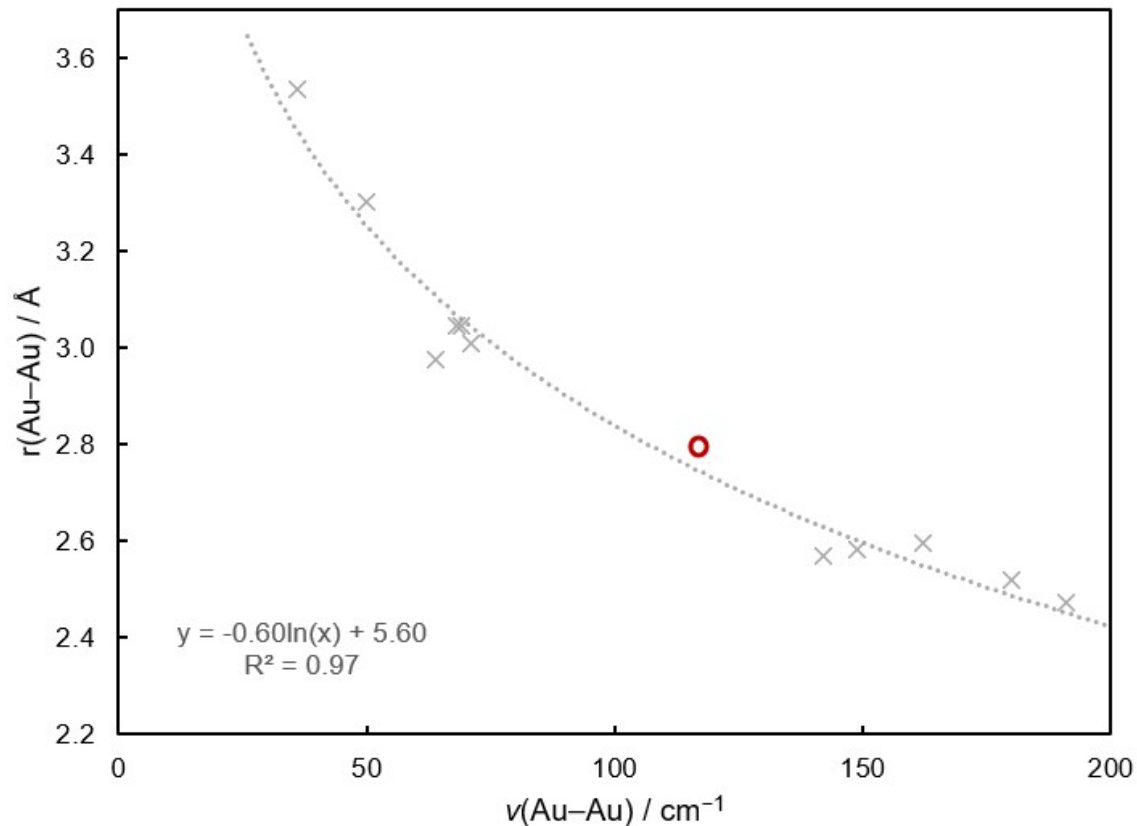


Figure S11. Plot of Au–Au distances and $\nu(\text{Au–Au})$ Raman stretching frequencies of **2** (red) and literature known complexes featuring Au–Au aurophilic interactions. See ref. 4 and references therein.

1.2.3 Reaction of {Fe(depe)₂}₂(C₂P₂Au₂) (2) with Me₃SiCl

A drop of Me₃SiCl (approx. 10 mg, 0.1 mmol) was added to a suspension of {Fe(depe)₂}₂(C₂P₂Au₂) (15 mg, 0.01 mmol) in benzene (1 mL), upon which the solution rapidly changes colour from deep red to pale yellow-brown. The reaction mixture was stirred for 1 h, during which time an insoluble brown precipitate forms. The solvent was removed under vacuum, and the resulting residue extracted with hexane (2 × 1 mL). The solution was concentrated, then stored at –35 °C for 2 days, during which Fe(depe)₂(Cl)(CP) crystallizes as yellow blocks. Isolated yield: 4 mg, 0.01 mmol, 35%. NMR characterization was consistent with previously reported data.

1.3 Cyclic voltammetry

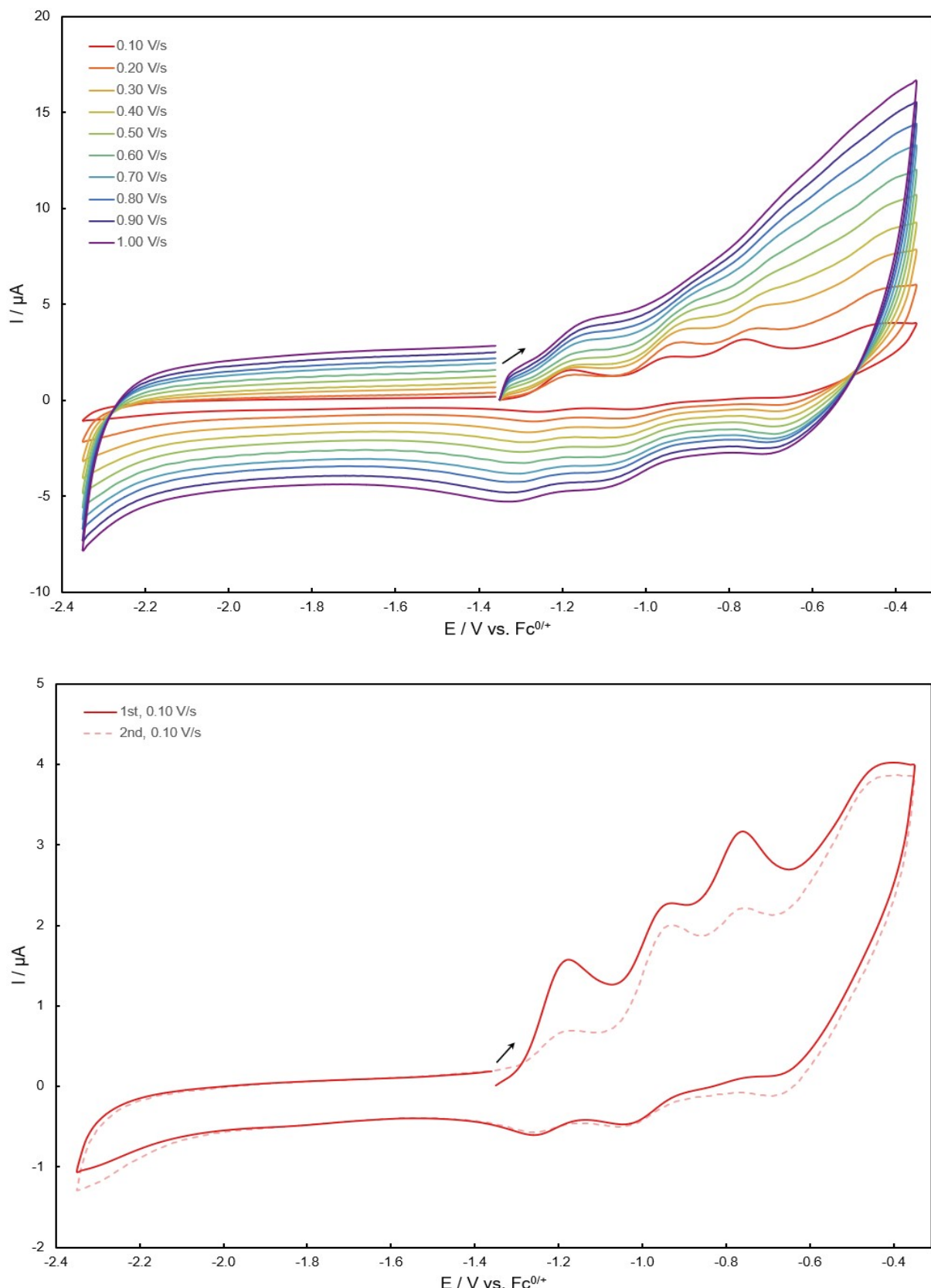


Figure S12. Cyclic voltammograms (THF, 0.2 M $[\text{NBu}_4]\text{[PF}_6]$) of **2** (0.1 mM), scanned anodically from -2.35 to -0.35 V at varying scan rates (0.10–1.00 V/s) (top), and twice at 1.00 V/s (bottom). All potentials were referenced to $\text{Fc}^{+/-}$.

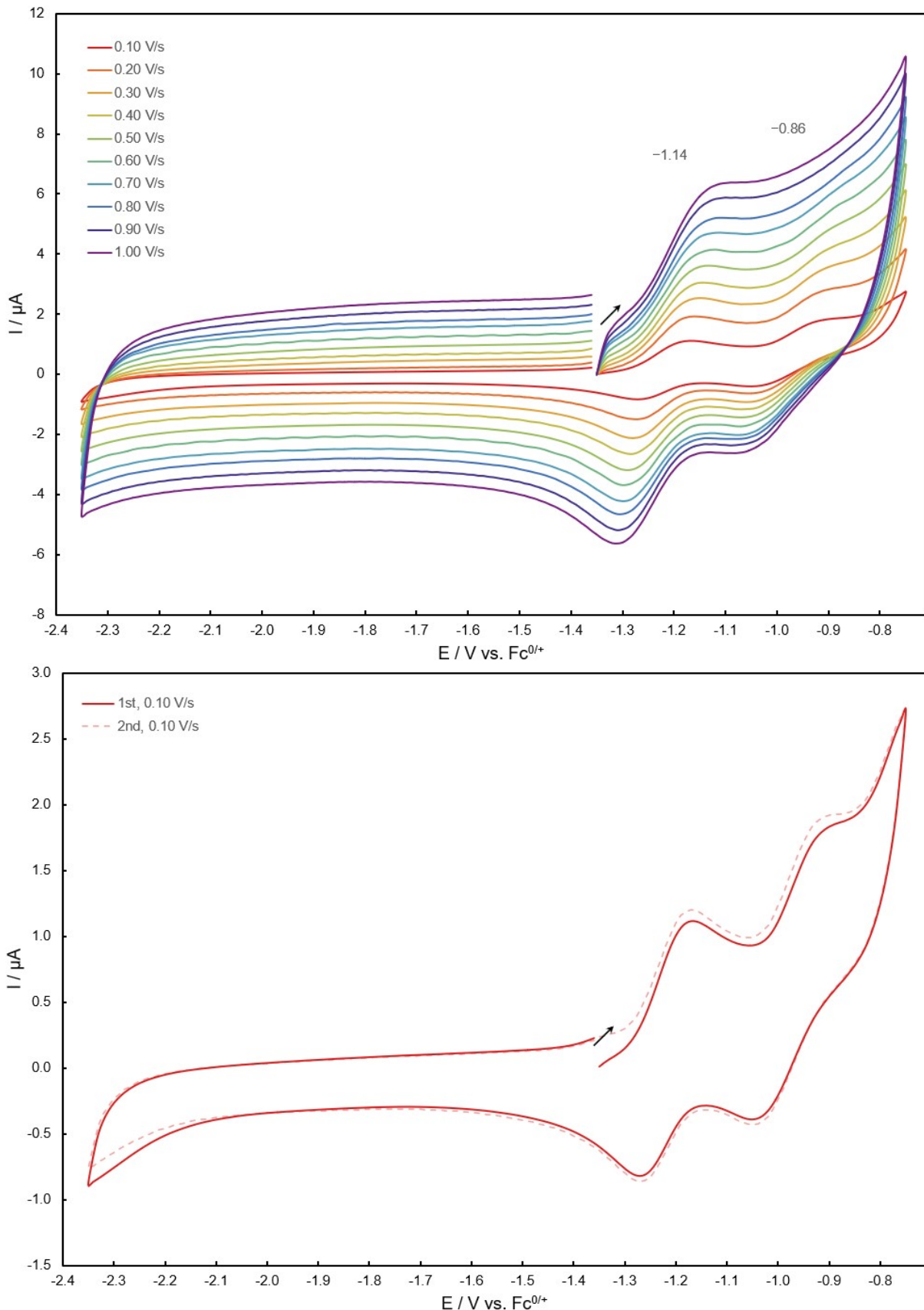


Figure S13. Cyclic voltammograms (THF, 0.2 M $[\text{NBu}_4]\text{[PF}_6]$) of **2** (0.1 mM), scanned anodically from -2.35 to -0.75 V at varying scan rates (0.10–1.00 V/s) (top), and twice at 1.00 V/s (bottom). All potentials were referenced to $\text{Fc}^{+/\text{0}}$.

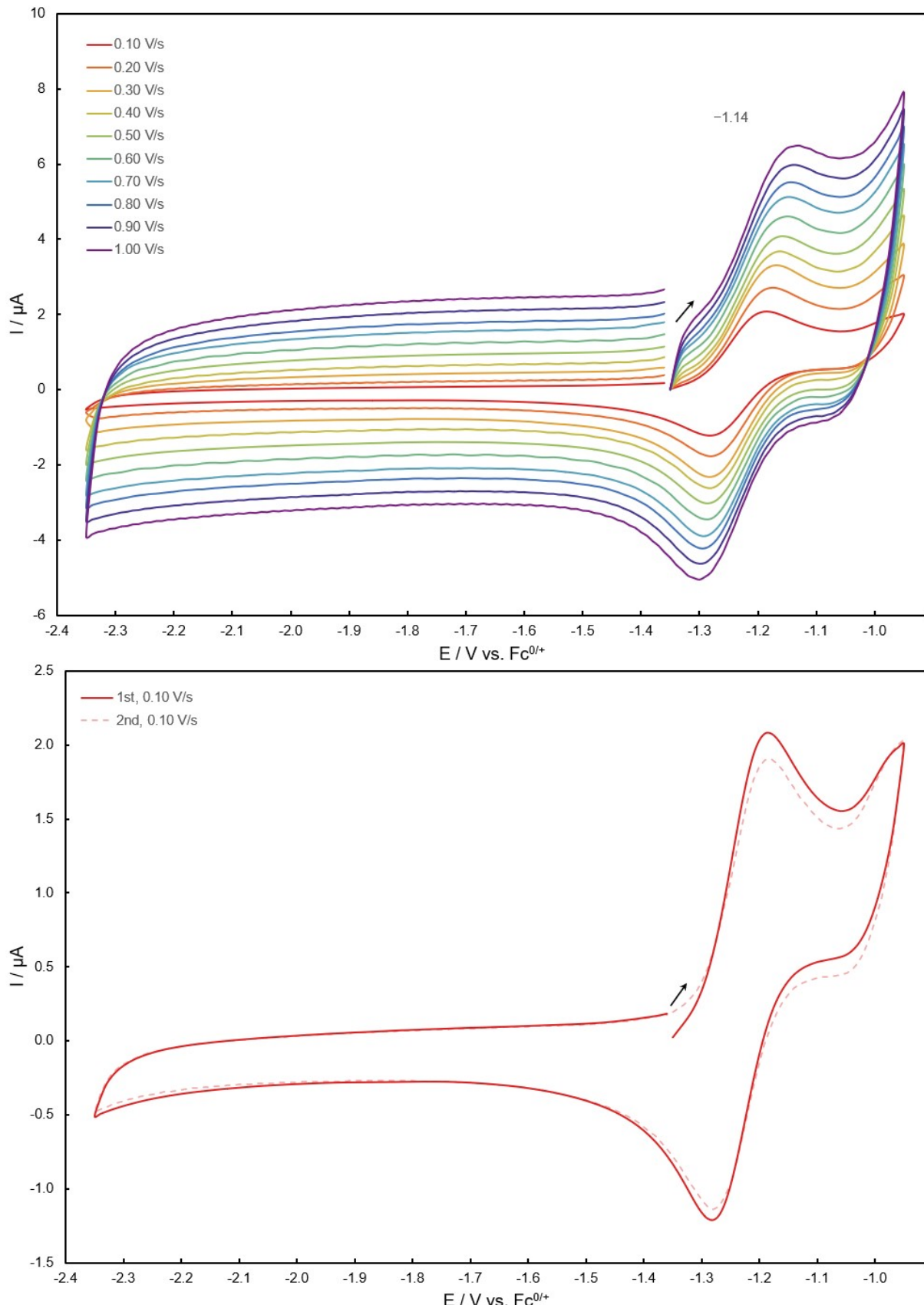


Figure S14. Cyclic voltammograms (THF, 0.2 M $[\text{NBu}_4]\text{[PF}_6]$) of **2** (0.1 mM), scanned anodically from -2.35 to -0.95 V at varying scan rates (0.10–1.00 V/s) (top), and twice at 1.00 V/s (bottom). All potentials were referenced to $\text{Fc}^{+/\circ}$.

2. Single crystal X-ray diffraction data

Single-crystal X-ray diffraction data were collected using an Oxford Diffraction Supernova dual-source diffractometer equipped with a 135 mm Atlas CCD area detector. Crystals were selected under Paratone-N oil, mounted on micro-mount loops and quench-cooled using an Oxford Cryosystems open flow N₂ cooling device. Data were collected using mirror monochromated Cu K α ($\lambda = 1.54184 \text{ \AA}$) radiation and processed using the CrysAlisPro package, including unit cell parameter refinement and inter-frame scaling (which was carried out using SCALE3 ABSPACK within CrysAlisPro).⁵ Structures were subsequently solved using direct methods and refined on F^2 using the SHELXL package.⁶

Table S1. Selected X-ray data collection/refinement parameters for **1·tol** and **2·2C₆H₆**.

	1·tol	2·2C₆H₆
Formula	C ₆₄ H ₈₅ AuGaN ₄ P	C ₅₄ H ₁₀₈ Au ₂ Fe ₂ P ₁₀
CCDC	2402916	2402917
Fw [g mol ⁻¹]	1208.01	1572.73
Crystal system	monoclinic	triclinic
Space group	<i>P</i> 2 ₁ / <i>n</i>	<i>P</i> –1
<i>a</i> (Å)	12.7127(1)	9.8473(2)
<i>b</i> (Å)	22.9597(2)	13.0366(3)
<i>c</i> (Å)	21.0072(2)	13.6086(4)
α (°)	90	81.050(2)
β (°)	98.5020(10)	74.529(2)
γ (°)	90	76.115(2)
<i>V</i> (Å ³)	6064.19(9)	1626.66(7)
<i>Z</i>	4	1
Radiation, λ (Å)	Cu K α , 1.54184	Cu K α , 1.54184
Temp (K)	150(2)	150(2)
ρ_{calc} (g cm ⁻³)	1.323	1.605
μ (mm ⁻¹)	5.572	14.356
Reflections collected	67534	36191
Indep. reflections	12642	6750
Parameters	728	315
R(int)	0.0353	0.0418
R1/wR2, ^[a] $ I \geq 2\sigma I $ (%)	2.11/5.05	2.72/6.76
R1/wR2, ^[a] all data (%)	2.43/5.23	2.85/6.87
GOF	1.059	1.019

^[a] R1 = $[\sum |F_o| - |F_c|]/\sum |F_o|$; wR2 = $\{[\sum w(|F_o|^2 - |F_c|^2)^2]/[\sum w(|F_o|^2)^2]\}^{1/2}$; w = $[\sigma^2(F_o)^2 + (AP)^2 + BP]^{-1}$, where P = $[(F_o)^2 + 2(F_c)^2]/3$ and the A and B values are 0.0248 and 2.58 for **1·tol**, and 0.0380 and 3.93 for **2·2C₆H₆**.

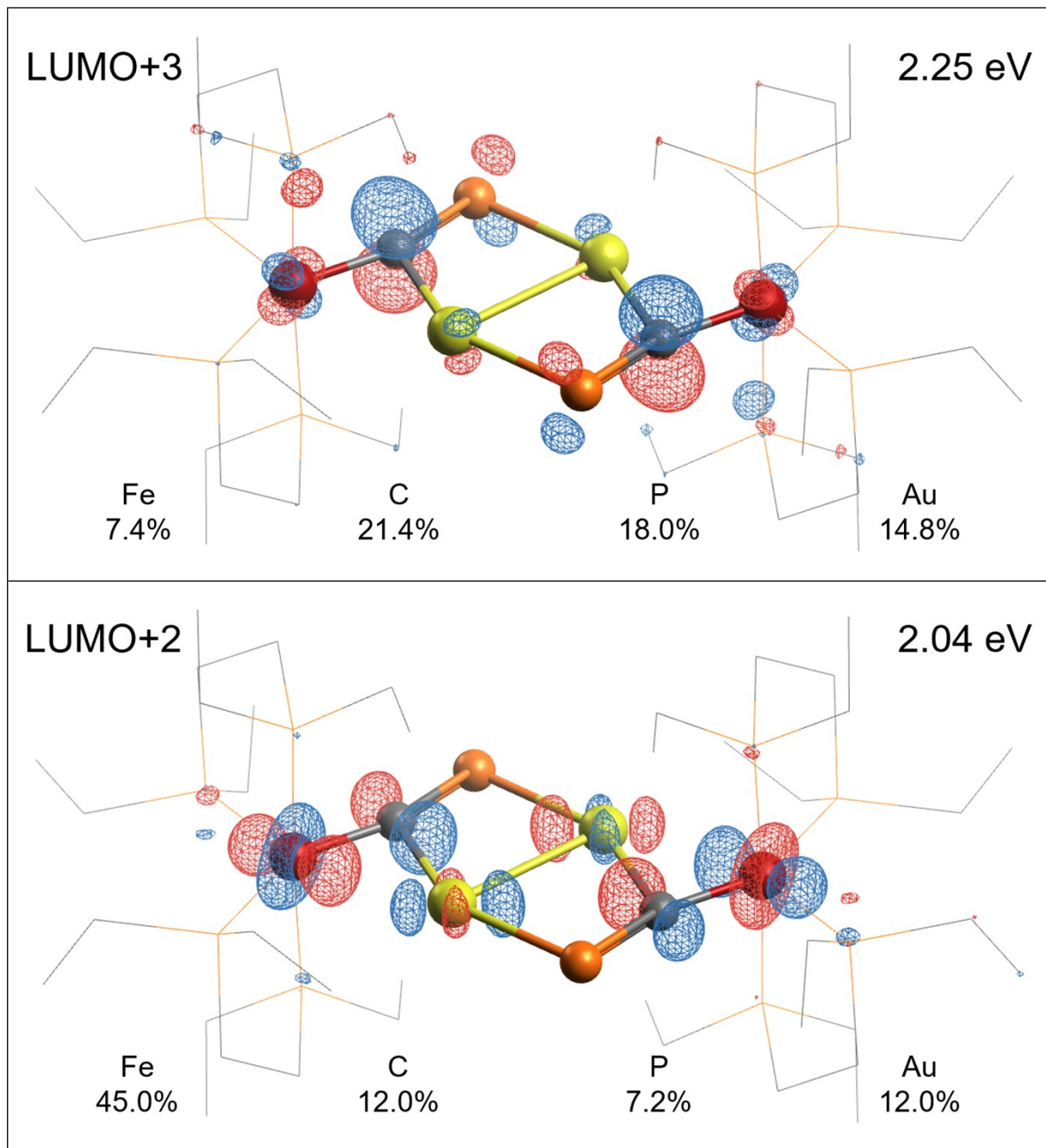
3. Computational details

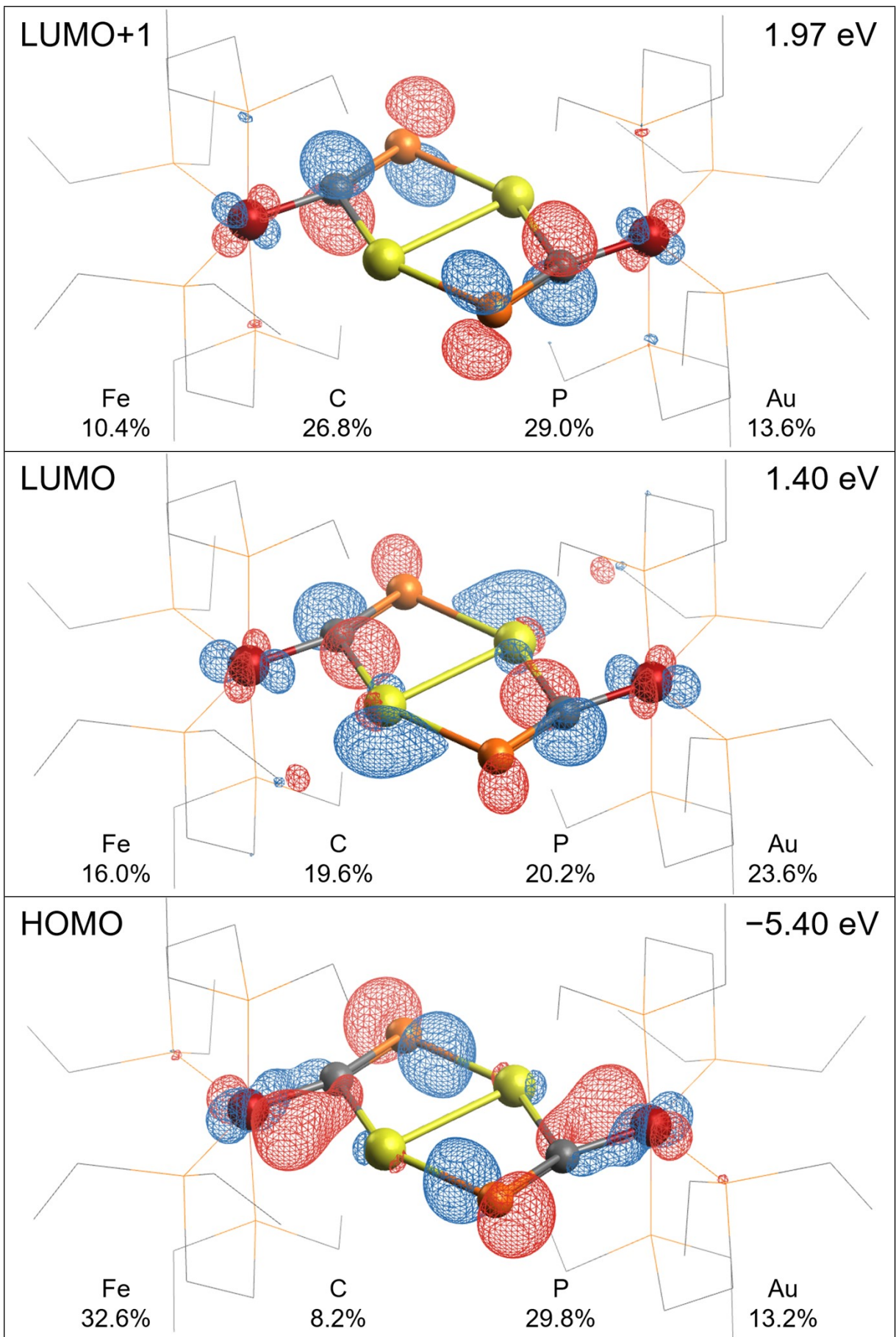
3.1. General computational methods

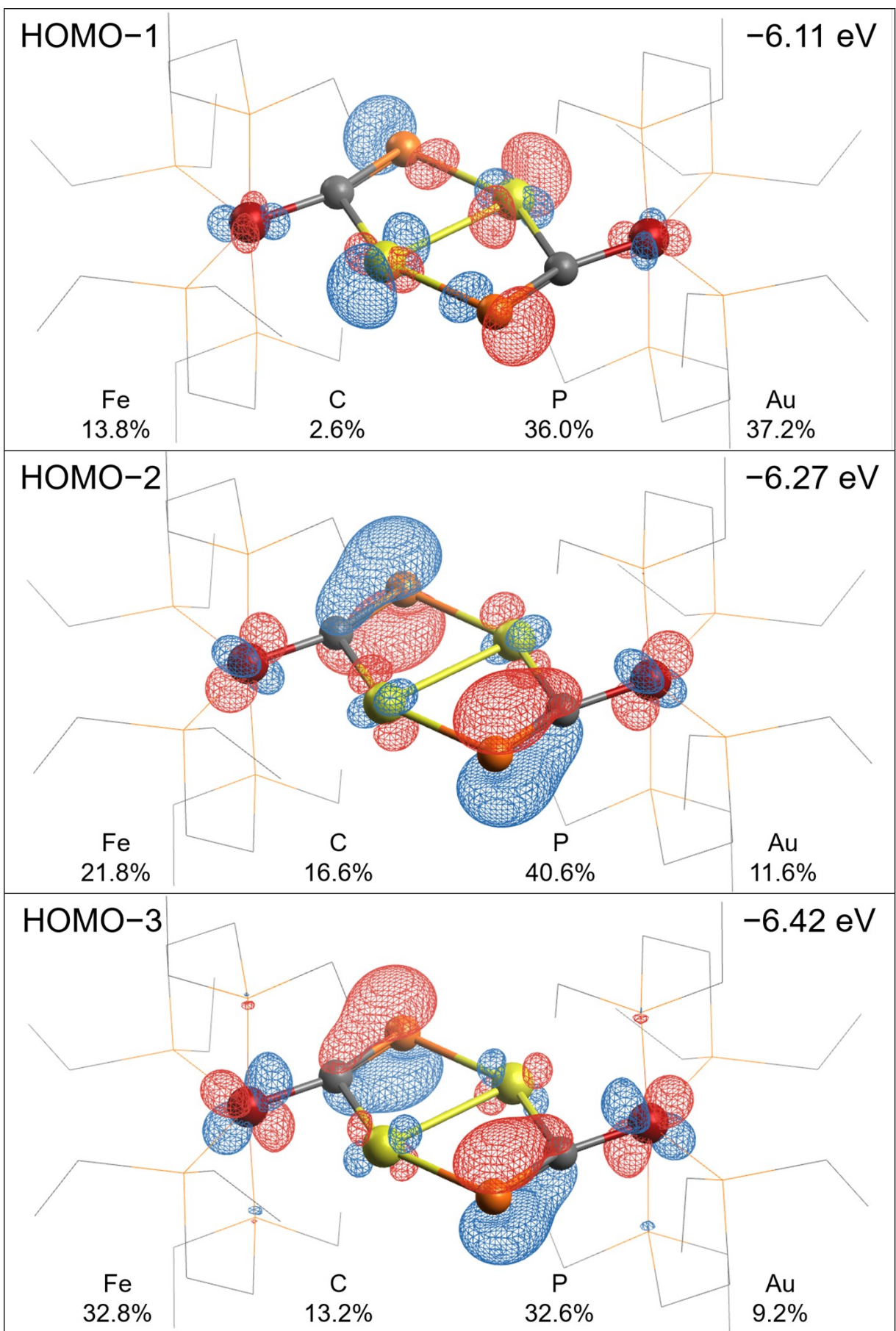
Density functional theory (DFT) calculations were performed using the ORCA 5.0.2 software package.⁷⁻⁹ All methods were used as implemented. Geometries were optimized using the B97-D3 functional and the def2-SVP basis set.^{10,11} Analytical frequency calculations were carried out to verify all geometries as true minima ($N_{\text{imag}} = 0$). Single point calculations were performed using the ωB97X-D3 functional¹² and the Resolution of Identity approximation (RIJCOSX),^{13,14} and corrected for relativistic effects using the zeroth order regular approximation (ZORA). The segmented all-electron relativistically contracted basis set SARC-ZORA-TZVPP was used for Au, and the relativistically contracted triple-zeta basis set ZORA-def2-TZVPP was used for all other atoms, along with the SARC/J auxiliary basis set.^{15,16} Quantum Theory of Atoms in Molecules (QTAIM) topology analysis was carried out using Multiwfn 3.8.¹⁷

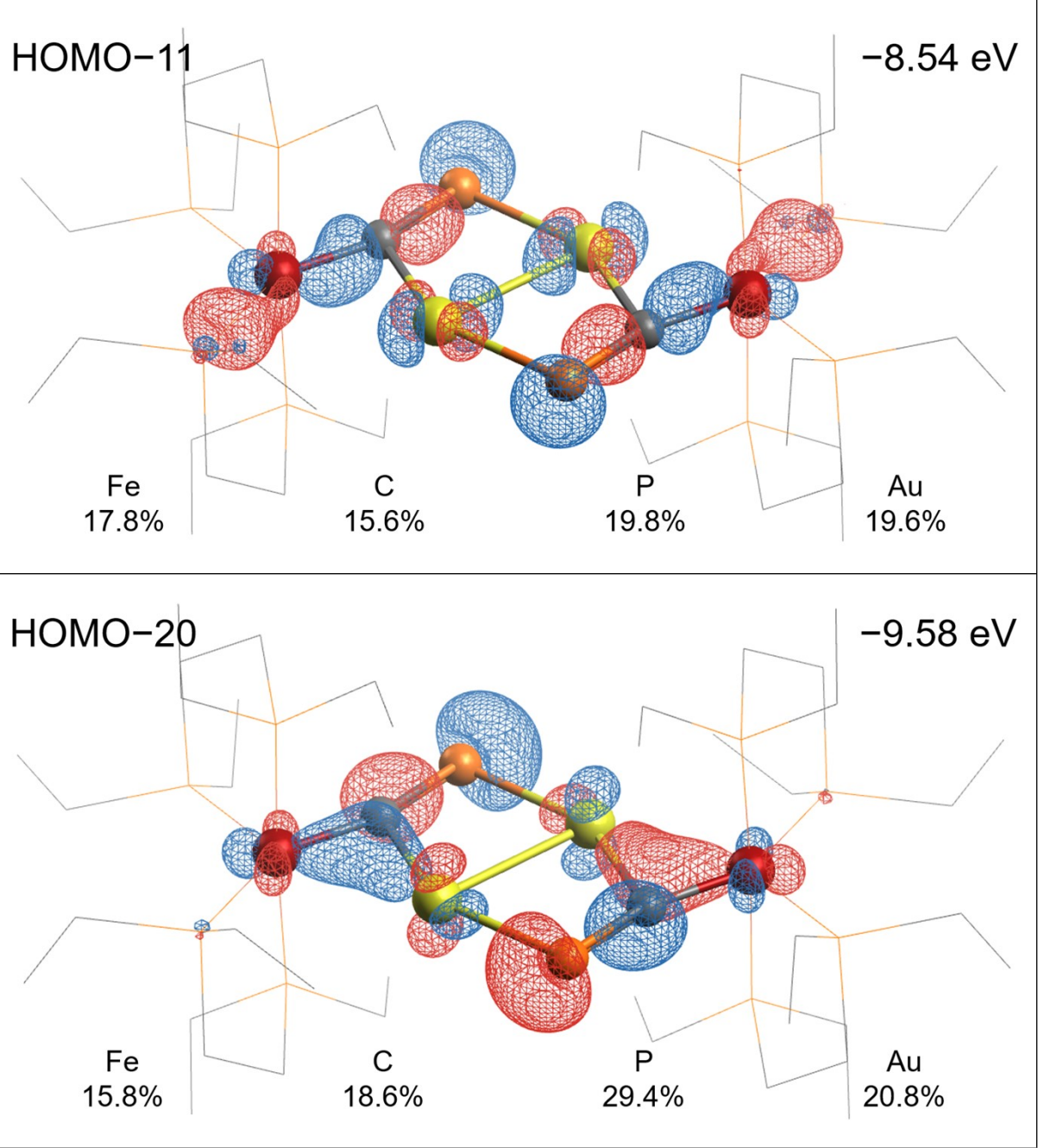
3.2. Electronic structure calculations

Table S2. Selected molecular orbital isosurface plots and per-MO Loewdin reduced orbital populations for **2**.









3.3. Topological Analysis

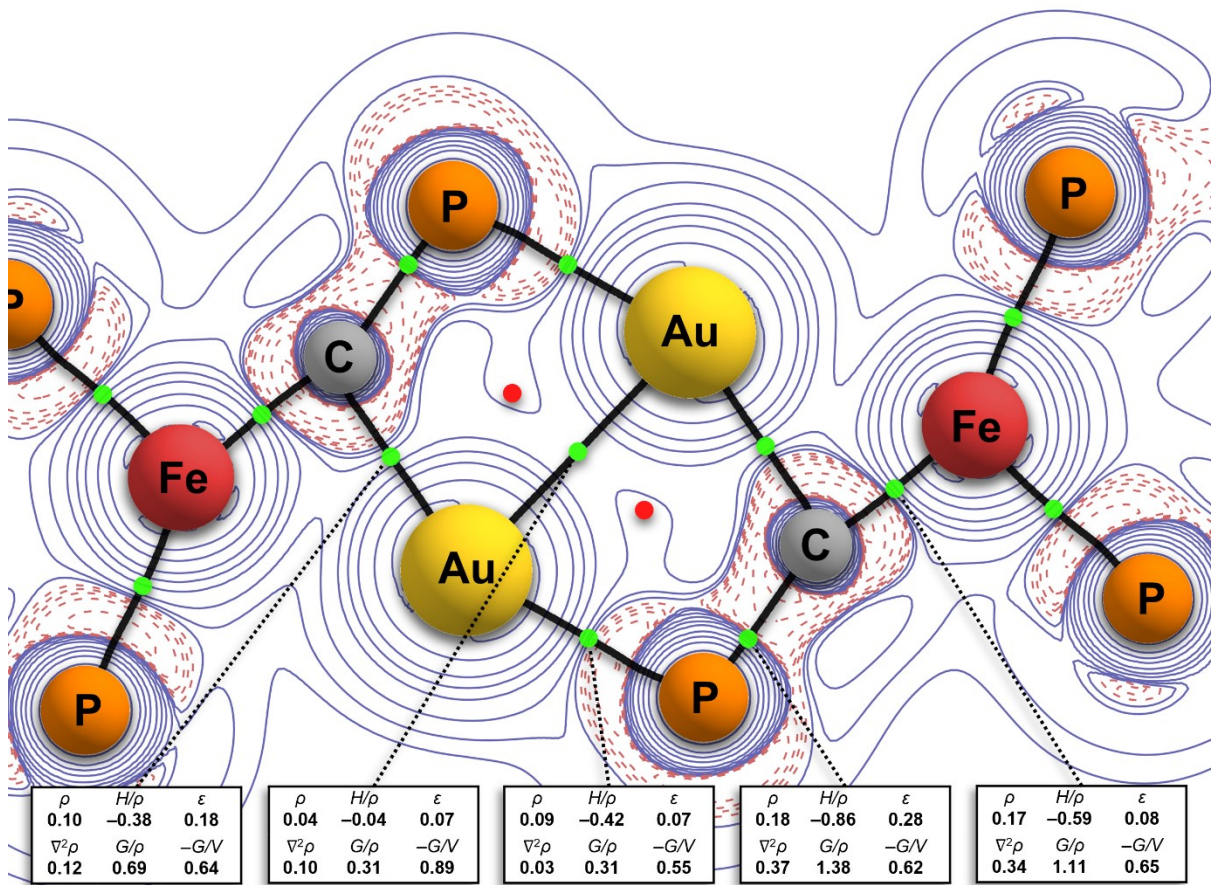


Figure S15. 2D Quantum Theory of Atoms in Molecules (QTAIM) analysis of **2**. Contour lines show the Laplacian of the electron density ($\nabla^2\rho$) (blue $\nabla^2\rho > 0$; red $\nabla^2\rho < 0$). Atomic critical points (3, +3) are displayed as atom labels. Bond critical points (3, -1) are displayed as green dots. Bond paths are displayed as black lines. The values of the electron density (ρ), the Laplacian of the electron density ($\nabla^2\rho$), the relative energy density (H/ρ), the relative kinetic energy density (G/ρ), the ratio of kinetic and potential energy densities ($-G/V$), and the ellipticity (ε) at each bond critical point are given in atomic units (a.u.).

3.4. XYZ coordinates

{Fe(depe) ₂ (C ₂ P ₂ Au ₂) (2)}							
Fe	-3.55349	-0.04281	0.02884	H	-3.09252	2.65676	-1.99021
Fe	3.55412	0.04277	-0.02885	H	-4.11041	2.39416	-3.43285
C	-2.07691	0.95274	0.04753	C	-5.21007	2.42183	-1.53131
C	2.07756	-0.95281	-0.04757	H	-6.11074	1.98939	-1.99661
P	-0.99956	2.25271	0.04226	H	-5.39088	3.49916	-1.42766
P	1.00021	-2.25277	-0.04233	C	-2.07636	0.13657	-3.23982
Au	-1.06206	-1.00518	-0.02788	H	-2.25763	0.71666	-4.15868
Au	1.06269	1.00510	0.02787	H	-1.27635	0.64648	-2.68218
P	-4.51839	-2.07461	-0.04705	C	-1.68270	-1.30437	-3.56503
P	-3.38523	-0.45086	2.20955	H	-1.36212	-1.83234	-2.65433
P	-3.58572	0.30837	-2.16062	H	-0.84155	-1.32137	-4.27186
P	-5.01461	1.57945	0.15534	H	-2.50881	-1.86883	-4.02457
C	-4.39607	-2.93487	1.63662	C	-4.93491	-0.46670	-3.21877
H	-5.35680	-2.77515	2.15076	H	-4.82323	-1.55660	-3.13777
H	-4.27481	-4.02016	1.51354	H	-5.87598	-0.22372	-2.70296
C	-3.26352	-2.30731	2.44333	C	-5.00600	-0.05216	-4.69149
H	-2.27855	-2.59444	2.04633	H	-5.14859	1.03234	-4.80554
H	-3.30380	-2.58496	3.50753	H	-5.85190	-0.54900	-5.19320
C	-6.38100	-2.23927	-0.33680	C	-6.84030	1.39070	0.59237
H	-6.82572	-1.50219	0.34895	H	-7.24209	0.68684	-0.15365
H	-6.57171	-1.86242	-1.35290	H	-6.88246	0.86967	1.55985
C	-7.03911	-3.60937	-0.13884	C	-7.68681	2.66754	0.63588
H	-6.64677	-4.36348	-0.83686	H	-7.33864	3.35762	1.41813
H	-8.12671	-3.54654	-0.30575	H	-8.74172	2.43195	0.85180
H	-6.88544	-3.99132	0.88110	H	-7.65834	3.20709	-0.32204
C	-3.87405	-3.40076	-1.22954	C	-4.49446	2.98324	1.30915
H	-4.68835	-4.10879	-1.44789	H	-5.10646	2.89055	2.22073
H	-3.64852	-2.87144	-2.16398	H	-3.46286	2.73276	1.58063
C	-2.62514	-4.15448	-0.76900	C	-4.52271	4.42066	0.78637
H	-1.82053	-3.45129	-0.50323	H	-3.83403	4.53795	-0.06286
H	-2.25054	-4.80494	-1.57452	H	-4.18262	5.11192	1.57448
H	-2.82586	-4.79077	0.10520	H	-5.52532	4.74434	0.47022
C	-4.86263	-0.06904	3.31412	P	4.51891	2.07462	0.04715
H	-5.00136	1.02023	3.27164	P	3.38584	0.45092	-2.20955
H	-5.73157	-0.50255	2.79671	P	3.58635	-0.30853	2.16060
C	-4.81287	-0.53953	4.77086	P	5.01531	-1.57942	-0.15543
H	-4.74318	-1.63452	4.84646	C	4.39657	2.93495	-1.63649
H	-5.72390	-0.23181	5.30918	H	5.35732	2.77530	-2.15061
H	-3.95360	-0.11266	5.30795	H	4.27527	4.02023	-1.51336
C	-1.96362	0.15446	3.25870	C	3.26407	2.30738	-2.44324
H	-1.90277	-0.51482	4.13161	H	2.27908	2.59447	-2.04626
H	-1.06467	-0.01682	2.64884	H	3.30437	2.58509	-3.50743
C	-2.03748	1.62090	3.69131	C	6.38150	2.23942	0.33695
H	-1.86153	2.28155	2.83166	H	6.82631	1.50239	-0.34879
H	-1.26168	1.83839	4.44041	H	6.57221	1.86256	1.35306
H	-3.00671	1.88141	4.14163	C	7.03950	3.60958	0.13904
C	-3.97585	2.12378	-2.37484	H	6.64699	4.36366	0.83700

H	8.12709	3.54686	0.30608	C	2.07698	-0.13689	3.23980
H	6.88592	3.99149	-0.88093	H	2.25828	-0.71704	4.15861
C	3.87446	3.40064	1.22974	H	1.27700	-0.64682	2.68212
H	4.68875	4.10861	1.44831	C	1.68321	1.30400	3.56511
H	3.64878	2.87118	2.16406	H	1.36260	1.83201	2.65445
C	2.62563	4.15448	0.76915	H	0.84205	1.32088	4.27193
H	1.82102	3.45136	0.50319	H	2.50926	1.86848	4.02470
H	2.25096	4.80483	1.57472	C	4.93550	0.46657	3.21879
H	2.82647	4.79089	-0.10493	H	4.82375	1.55646	3.13785
C	4.86323	0.06920	-3.31416	H	5.87658	0.22368	2.70294
H	5.00208	-1.02005	-3.27163	C	5.00664	0.05193	4.69147
H	5.73215	0.50282	-2.79679	H	5.14935	-1.03256	4.80545
C	4.81337	0.53962	-4.77091	H	5.85248	0.54883	5.19322
H	4.74354	1.63459	-4.84658	H	4.09280	0.32782	5.23690
H	5.72443	0.23199	-5.30924	C	6.84098	-1.39053	-0.59246
H	3.95415	0.11260	-5.30796	H	7.24272	-0.68663	0.15355
C	1.96424	-0.15439	-3.25871	H	6.88310	-0.86950	-1.55995
H	1.90336	0.51491	-4.13160	C	7.68761	-2.66730	-0.63597
H	1.06528	0.01684	-2.64884	H	7.33954	-3.35739	-1.41824
C	2.03814	-1.62082	-3.69136	H	8.74250	-2.43161	-0.85184
H	1.86224	-2.28150	-2.83172	H	7.65915	-3.20687	0.32194
H	1.26232	-1.83832	-4.44044	C	4.49522	-2.98319	-1.30929
H	3.00736	-1.88127	-4.14171	H	5.10718	-2.89042	-2.22087
C	3.97658	-2.12393	2.37471	H	3.46359	-2.73275	-1.58073
H	3.09329	-2.65693	1.99004	C	4.52355	-4.42064	-0.78658
H	4.11115	-2.39436	3.43271	H	3.83488	-4.53803	0.06263
C	5.21083	-2.42186	1.53118	H	4.18352	-5.11188	-1.57473
H	6.11147	-1.98938	1.99649	H	5.52619	-4.74426	-0.47044
H	5.39172	-3.49918	1.42748				

4. References

- 1 D. W. N. Wilson, S. J. Urwin, E. S. Yang and J. M. Goicoechea, *J. Am. Chem. Soc.*, 2021, **143**, 10367–10373.
- 2 N. J. Hardman, B. E. Eichler and P. P. Power, *Chem. Commun.*, 2000, 1991–1992.
- 3 P. J. Hill, L. R. Doyle, A. D. Crawford, W. K. Myers and A. E. Ashley, *J. Am. Chem. Soc.*, 2016, **138**, 13521–13524.
- 4 D. Perreault, M. Drouin, A. Michel, V. M. Miskowski, W. P. Schaefer and P. D. Harvey, *Inorg. Chem.*, 1992, **31**, 695–702.
- 5 *CrysAlisPro*, Agilent Technologies, Version 1.171.42.57a.
- 6 G. M. Sheldrick, *Acta Crystallogr. Sect. C*, 2015, **71**, 3–8.
- 7 F. Neese, *Wiley Interdiscip. Rev. Comput. Mol. Sci.*, 2012, **2**, 73–78.
- 8 F. Neese, *Wiley Interdiscip. Rev. Comput. Mol. Sci.*, 2018, **8**, 1–6.
- 9 F. Neese, F. Wennmohs, U. Becker and C. Ripplinger, *J. Chem. Phys.*, 2020, **152**, 224108.
- 10 S. Grimme, *J. Comput. Chem.*, 2006, **27**, 1787–1799.
- 11 F. Weigend and R. Ahlrichs, *Phys. Chem. Chem. Phys.*, 2005, **7**, 3297–3305.
- 12 Y. S. Lin, G. De Li, S. P. Mao and J. Da Chai, *J. Chem. Theory Comput.*, 2013, **9**, 263–272.
- 13 F. Neese, F. Wennmohs, A. Hansen, U. Becker, *Chem. Phys.*, 2009, **356**, 98–109.
- 14 R. Izsák, F. Neese, *J. Chem. Phys.*, 2011, **135**, 144105.
- 15 D. A. Pantazis, X. Y. Chen, C. R. Landis and F. Neese, *J. Chem. Theory Comput.*, 2008, **4**, 908–919.
- 16 M. Bühl, C. Reimann, D. A. Pantazis, T. Bredow and F. Neese, *J. Chem. Theory Comput.*, 2008, **4**, 1449–1459.
- 17 T. Lu and F. Chen, *J. Comput. Chem.*, 2012, **33**, 580–592.